

## Ti/TiO<sub>2</sub>/Cu<sub>2</sub>O Based Electrodes as Photocatalysts in PEC Cells

Antonio Rubino\*, Pier G. Schiavi, Pietro Altimari, Alessandro Latini, Francesca Pagnanelli

Department of Chemistry, Sapienza University of Rome, P.le Aldo Moro 5, 00185, Rome, Italy.  
[antonio.rubino@uniroma1.it](mailto:antonio.rubino@uniroma1.it)

Composite Ti/TiO<sub>2</sub>/Cu<sub>2</sub>O electrodes were produced by electrodeposition of p-Cu<sub>2</sub>O nanoparticles over the surface of TiO<sub>2</sub> nanotubes generated by one-step electrochemical anodization of titanium. The effect of electrodeposition potential and duration of the electrodeposition experiments on size and morphology of the Cu<sub>2</sub>O nanoparticles was evaluated by FE-SEM analysis. In order to evaluate the photo-catalytic activity of the composite electrodes, photo-degradation experiments with methylene blue and photo-electrochemical tests were performed. An anodic current was generated by photo-electrochemical tests under visible light and zero bias, confirming the transfer of photo-generated electrons from Cu<sub>2</sub>O to TiO<sub>2</sub>. However, in both the photo-degradation and the photo-electrochemical experiments, the photo-catalytic activity of the composite electrodes under simulated solar irradiation (UV + visible) was lower as compared to the application of the bare TiO<sub>2</sub> nanotubes electrodes. The mechanisms that could justify such results are thoroughly discussed.

### 1. Introduction

The increasing atmospheric concentration of greenhouse gases raises serious concerns on fossil fuel energy supply (Beer et al., 2010). To date, increasing attention is given to systems' development for electric energy production from renewables (solar and wind). The intermittency of such energy sources imposes the recourse to energy storage technologies including batteries and accumulators. These technologies are however insufficient to guarantee the required autonomy in many applications.

A promising strategy to overcome this limit is the accumulation of the energy derived from renewables into chemicals, which can be used to generate power. In accordance with this idea, particular attention is paid to the application of the solar energy to produce hydrogen (high energy density, null environmental impact) (Momirlan and Veziroglu, 2005; Altimari et al., 2014).

Direct hydrogen production through solar energy application is possible using semiconductor based photocatalysts (Hisatomi et al, 2014) with the following two different approaches: photo-electrochemical water-splitting and photo-catalytic "reforming" of organics. In order to perform photo-electrochemical water splitting, the conduction and valence band of the photocatalyst should straddle the water reduction and oxidation potentials. Titanium dioxide TiO<sub>2</sub>, which is an n-type semiconductor, satisfies this requirement and is the most extensively investigated photocatalyst to perform water-splitting and photo-catalytic reforming. Considerable advantages are attained by the application of TiO<sub>2</sub> nanotubes (NTs), which can ensure an elevated surface to volume ratio and thus reduce charge carrier recombination and enhance process kinetics.

Electrochemical anodization of titanium is an effective and versatile method (e.g. near-room temperature conditions, aqueous solutions in most cases) to produce TiO<sub>2</sub> NTs. With such method, diameter, length and morphology of the NTs can be effectively controlled by varying the applied anodization potential and the electrolyte composition.

TiO<sub>2</sub> NTs have been proven to exhibit promising catalytic performances in many electrochemical reactions, such as OER and HER (Malgras et al. 2015), where the electrolyte diffusion can be tuned by tailoring the pore size of the porous materials: Macropores (>50nm) provide facile transfer and diffusion of reactants and products in the reaction over the electrodes.

Central limit to the application of TiO<sub>2</sub> is its wide band gap (i.e. 3.0-3.3 eV), which restricts the portion of the absorbed solar light to the UV irradiance range (5% of the irradiated solar energy). A strategy to overcome this limit and enhance the photo-activity is to couple TiO<sub>2</sub> with semiconductors which can absorb visible light.

Cuprous oxide is a p-type semiconductor with a narrow band gap (i.e. 2.1-2.6 eV), which allows to absorb visible light. Traditionally, Cu<sub>2</sub>O deposition techniques on nanostructured TiO<sub>2</sub> include the impregnation with a copper salt and subsequent calcination. This offers poor control on the size, shape and composition of the deposited particles determining the catalyst activity.

Improved control of shape and morphology can be attained by electrodeposition (Schiavi et al. 2015, 2016, 2018b). With this method, the morphology of the deposited particles can be readily modified by varying the electrode potential and the electrolyte concentration, while the particle size can be controlled by modifying the overall transferred charge (Altimari and Pagnanelli, 2016).

In this article, we analyze the synthesis of composite electrodes Ti/TiO<sub>2</sub>/Cu<sub>2</sub>O by electrochemical anodization of titanium followed by direct electrodeposition of Cu<sub>2</sub>O nanoparticles. Photo-catalytic activity of the produced electrodes is characterized by analyzing the process of methylene blue photo-degradation.

## 2. Materials and methods

### 2.1 TiO<sub>2</sub> based electrodes preparation

The anodization process was carried in a symmetric two electrodes jacketed glass cell, kept at room temperature ( $24.5 \pm 0.5$ ) °C and magnetically stirred.

Both electrodes were made of titanium (Alfa Aesar 99.5%, annealed, thickness 0.25mm) immersed in Ethylene Glycol (Alfa Aesar, 99+%) based electrolytes, with 0.3%wt NH<sub>4</sub>F (Alfa Aesar, 98% min.) and 1%v/v H<sub>2</sub>O content. The electrodes were connected with a power supply (Aim-TTi CPX200DP DC Power Supply Dual Outputs, 2 x 60 V/10 A 180 W) to close the circuit.

Prior to anodization, the titanium electrodes were just degreased by Acetone (VWR Prolabo Chemicals, 100%) in ultrasonic bath (Elma® S 10 Elmasonic, 220-240 V~, 30 W, 50-60 Hz).

The anodization was carried out following a one-step anodization method, where the applied potential (U) was imposed according two stages: a first potentiodynamic anodization where the applied potential grows linearly ( $0.5 \text{ V s}^{-1}$ ) up to 60 V, reached which a potentiostatic anodization took place for 1 hour. At the end of the anodization process, the electrodes were washed with acetone and then dried.

The tubes top morphology, depending on the electrolyte and applied potential, is strongly connected with the anodization time: the electrolyte's etching effect becomes predominant respect to the growth and an undesired nano-grass morphology cover the tubes. This is why the dried electrodes are sonicated in H<sub>2</sub>O bath for 20 minutes.

The TiO<sub>2</sub> resulting from anodization is amorphous, so the electrodes were thermally treated in a muffle furnace (Nabertherm B410, Tmax 1100 °C, 1.2 KW), in air flow with a heating rate of  $8 \text{ °C min}^{-1}$  up to 580 °C, reached which it is kept constant for 1 hour.

### 2.2 Cu<sub>2</sub>O electrodeposition

The composite TiO<sub>2</sub>/Cu<sub>2</sub>O electrodes were realized by electrodeposition in a three electrodes jacketed glass cell, magnetically stirred and kept at room temperature.

Ti/TiO<sub>2</sub> electrode was employed as working electrode, a platinum gauze (25 mm x 20 mm) was used as counter electrode, while an Ag/AgCl saturated electrode was the reference electrode.

The electrolyte is composed by CuSO<sub>4</sub> 0.4 M in Lactic Acid 3 M, and then pH is adjusted to 11.0 by the addition of NaOH 5 M.

The electrodeposition tests were carried out with an IVIUMnSTAT potentiostat by following a pulsed method. This method included the cyclic application of a cathodic pulse (A period,  $t_{on}$ ) followed by a zero-current period (B period,  $t_{off}$ ), as reported in Table 1 (Schiavi et al., 2018a). In any test, the duration of the electrodeposition was indirectly fixed by assigning the overall charge to be transferred (Q).

Table 1: Pulsed electrodeposition (PED) methods

Method	A period		B period		Transferred charge
	E <sub>A</sub> (V Vs Ag/AgCl)	t <sub>on</sub> (s)	I <sub>B</sub> (A)	t <sub>off</sub> (s)	Q (mC)
PED1	-0.6	0.5	0	5	100
PED2	-0.8	0.5	0	5	100
PED2	-0.8	0.5	0	5	400
PED2	-0.8	0.5	0	5	1200
PED3	-0.9	0.5	0	5	100

### 2.3 Photo-catalytic activity

The photo-degradation of methylene blue (MB) (Alpha Aesar, 1%w/v) was performed to evaluate the photo-catalytic activity of prepared electrodes. The experiments were carried out by immersing the electrode in a quartz cuvette magnetically stirred containing 10 mL of MB solution with an initial concentration of 6.25 mg/L. The mixture was first stirred for 30 minutes in the dark at room temperature to ensure that the adsorption equilibrium was reached. Then the reaction solution was illuminated with a sunlight-simulation lamp (OSRAM Ultra Vitalux 300W) with an incident light of  $100 \text{ mW cm}^{-2}$ , measured with a luxmeter (Gossen Mavolux digital). The experimental apparatus employed to carry out the tests was contained in a “black box” to ensure that no external light source could perturb the experiments.

Solution samples were collected at fixed time intervals, and the concentration of MB was determined by UV–vis spectroscopy (Varian Cary 50 Scan spectrophotometer). The self-degradation of methylene blue under the same conditions of the photo-degradation experiments was also collected. A calibration curve (not shown here) of MB solution was obtained at 664.1 nm wavelength at different concentrations prepared.

## 3. Results and discussions

### 3.1 Mesoporous $\text{TiO}_2$ NTs

The electrodes were analysed with a Zeiss Auriga Field Emission Scanning Electron Microscope and the ImageJ software was employed for the FE-SEM images processing.

The FE-SEM images reported in Figure 1 shows the bare  $\text{Ti/TiO}_2$  electrode (prior to the electrodeposition process).

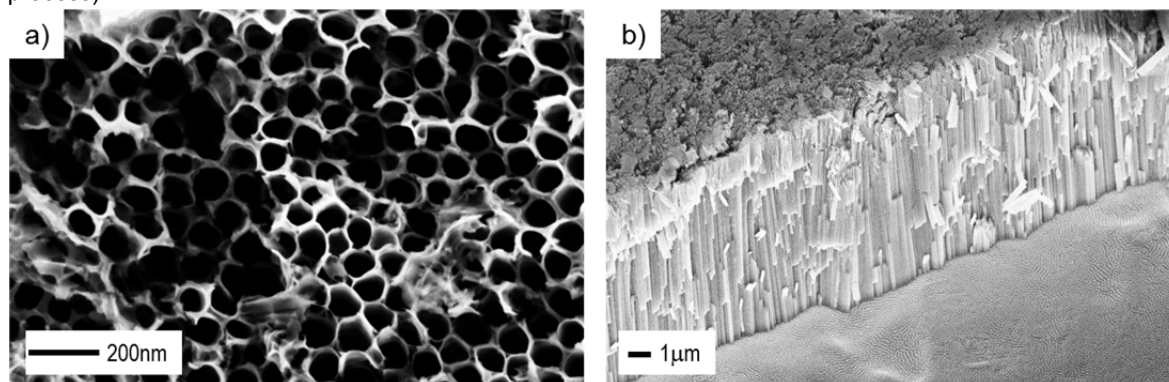


Figure 1: FE-SEM images – bare  $\text{Ti/TiO}_2$  electrode, a) “top view”; b) “cross sectional view”.

As reported by Macack et al (2007), the tube diameter ( $d$ ) can be computed as  $d = kU$ , where  $U$  is the applied potential during the anodization and  $k$  is a growth factor for anodic oxides. Typically, it is  $k \approx 1.3\text{-}3.3 \text{ nm V}^{-1}$  for  $\text{TiO}_2$  (Lu and Jiao, 2016) depending on the employed electrolyte.

The mean inner diameter estimated is coherent with this relation and is equal to 93.0 nm with the relative frequency distribution reported in Figure 2.

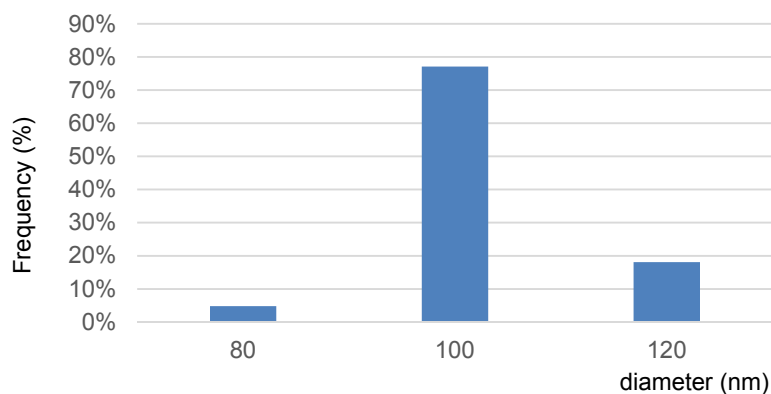


Figure 2:  $\text{Ti/TiO}_2$  electrode, inner tube diameter frequency distribution.

### 3.2 Composite TiO<sub>2</sub>/Cu<sub>2</sub>O electrodes

The composite TiO<sub>2</sub>/Cu<sub>2</sub>O electrodes were characterized by FE-SEM analysis. Top-view and cross-sectional images of the composite electrodes generated for different values of the charge Q imposed during the Cu<sub>2</sub>O electrodeposition are reported in Figure 3. It is apparent from this figure that increasing the transferred charge determines an increase in the dimensions of Cu<sub>2</sub>O nanoparticles. Even though not shown in Figure 3, we found that the transition from less cathodic to more cathodic electrodeposition potential induces a morphological transition from octahedral to spherical deposits.

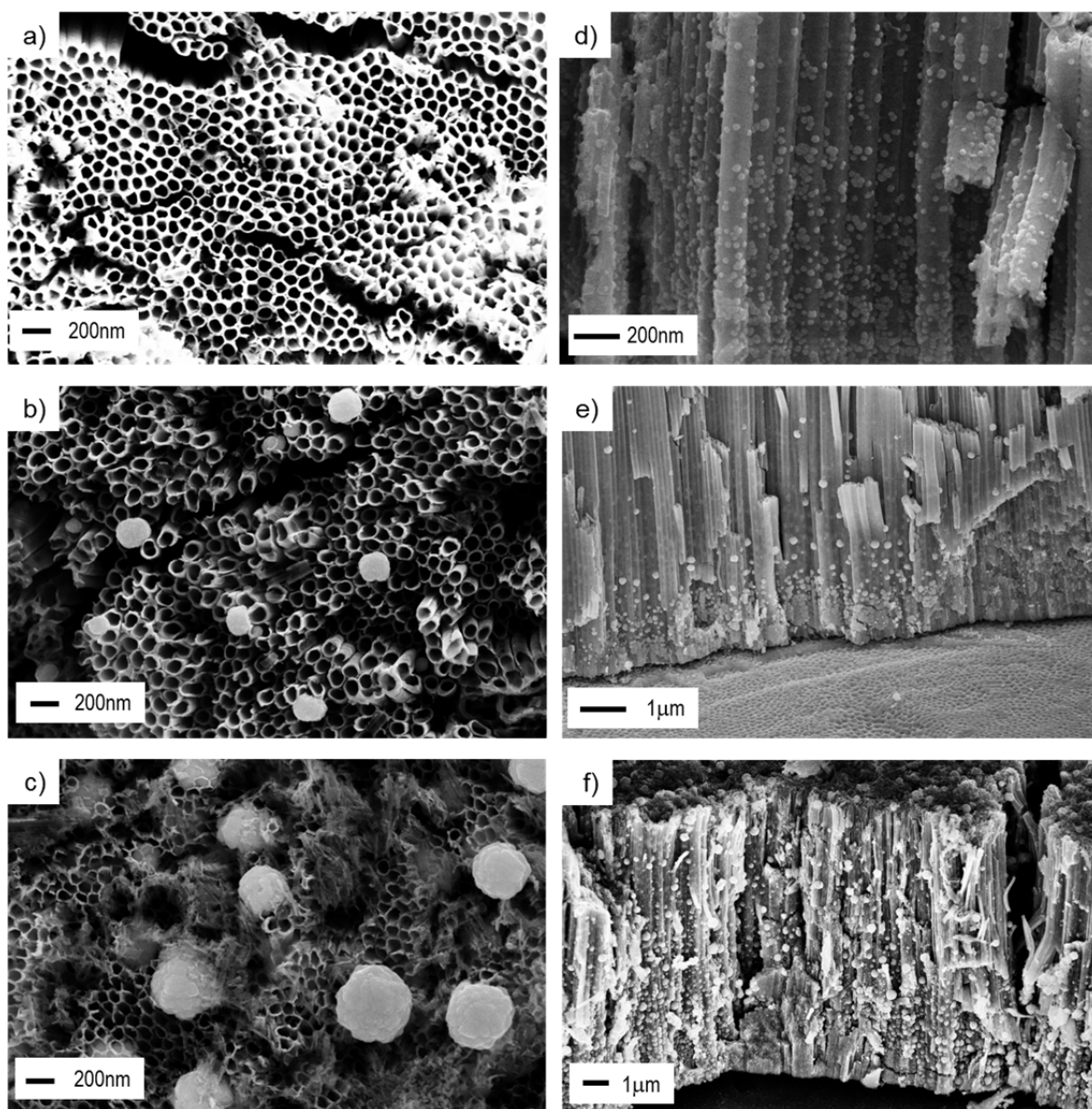


Figure 3: FE-SEM images – Composite TiO<sub>2</sub>/Cu<sub>2</sub>O electrodes obtained for electrodeposition method PED2 (table 1) a,b,c) and d,e,f) are the “topview” and “cross sectional view” respectively. The samples are obtained for different amount of transferred charge: a,d) 100 mC; b,e) 400 mC; c,f) 1200 mC.

### 3.3 Methylene blue photo-degradation tests

In order to evaluate the photo-activity of the produced electrodes, photo-degradation tests of methylene blue (MB) were carried out.

The diagrams reported in Figure 4 show the comparison between the evolutions of the MB concentration observed with the bare TiO<sub>2</sub> electrode and with the composite electrodes. The self-degradation of MB is also reported, and the activity is estimated as the ratio between the final and initial MB concentration ( $C_0$ ).

Results are not in line with expectations, the activity of the bare Ti/TiO<sub>2</sub> electrode being enhanced as compared to the composite electrodes. In particular, we can observe a decrease in the composite electrode activity with the increase of deposit dimensions (Figure 4a). The influence of the electrodeposition potential, (which is applied during the t<sub>ON</sub> period) was separately investigated. This evidenced that, maintaining constant the charge Q, a decrease in the composite electrode activity is attained when transition from an octahedral to a spherical Cu<sub>2</sub>O particle morphology is induced by increasing the cathodic potential (Figure 4b).

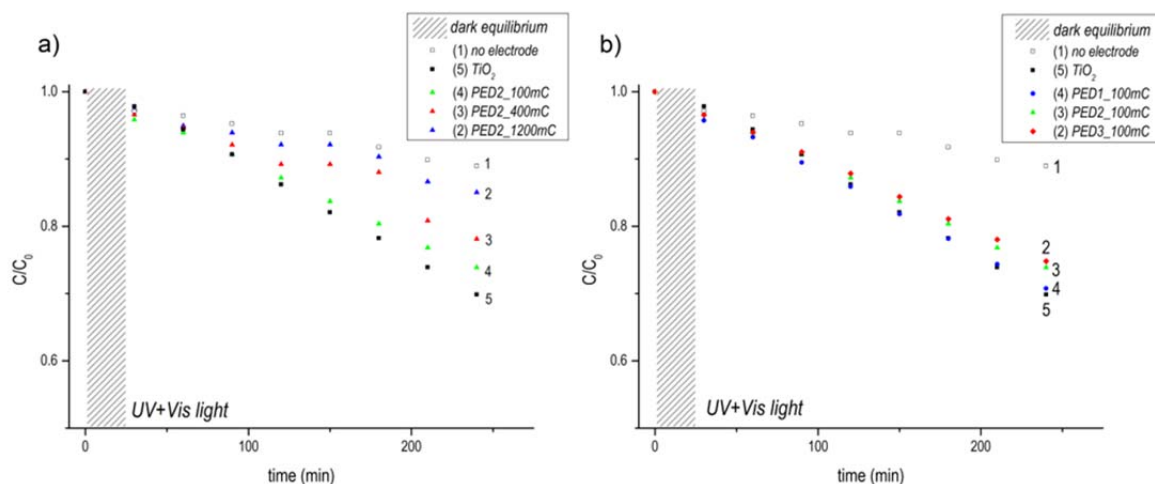


Figure 4: MB photo-degradation test. a) Comparison between electrodes synthesized for fixed electrodeposition potential (method PED2, -0.8V), increasing transferred charge: (1) no electrode; (2) Q=1200 mC; (3) Q=400 mC; (4) Q=100mC; (5) bare TiO<sub>2</sub> electrode. b) Comparison between electrodes synthesized for fixed transferred charge (100mC), varying electrodeposition potential: (1) no electrode; (2) method PED3 (-0.9V); (3) method PED2 (-0.8V); (4) method PED1 (-0.6V); (5) bare TiO<sub>2</sub> electrode.

In order to investigate the mechanisms responsible for the progressively deteriorating performances of the composite electrodes with increasing the transferred charge Q (equivalently, the amount of electrodeposited Cu<sub>2</sub>O), the composite electrodes were employed in a photo-electrochemical cell as working electrodes under 300 W Xe lamp irradiation (Solar Simulator HAL-320 ASAHI SPECTRA).

The photocurrent density generated under chopped UV + visible and only visible irradiation (presence of an UV filter,  $\lambda > 400$  nm) was recorded (data not shown). Chopped light irradiation was used in any experiment.

Under UV + visible irradiation, the anodic photocurrent for composite electrodes was still lower than that found with the bare TiO<sub>2</sub> electrode, while, under only visible irradiation, the composite electrode showed a higher anodic photocurrent as compared to the bare TiO<sub>2</sub> electrode.

The results of the photo-electrochemical tests performed under visible light radiation confirm that the composite TiO<sub>2</sub>/Cu<sub>2</sub>O electrode indeed follows the operation of a p-n junction with the photo-generated electrons being transferred from the Cu<sub>2</sub>O to TiO<sub>2</sub> and the photo-generated holes moving into the opposite direction from TiO<sub>2</sub> to Cu<sub>2</sub>O. In order to verify it, we remark that TiO<sub>2</sub> is not photoactive under visible light and that Cu<sub>2</sub>O alone (without TiO<sub>2</sub>) would generate a photo-cathodic current. We observed in contrast that illumination of the TiO<sub>2</sub>/Cu<sub>2</sub>O electrode was accompanied by the generation of a photo-anodic current, which corroborates the illustrated p-n junction operation. On the other hand, the tests performed under UV + visible light confirmed the lower performances of the composite electrodes as compared to the bare TiO<sub>2</sub>.

It is important to remark at this stage that very few previous studies (Sang et al., 2015) have demonstrated the possibility to improve the photo-catalytic performance of TiO<sub>2</sub> nanotubes under UV + visible light by the electrodeposition of Cu<sub>2</sub>O nanoparticles. The application of the composite electrodes generated by Cu<sub>2</sub>O electrodeposition has been typically analysed under only visible light irradiation. This invariably improves the photo-catalytic performance as compared to the bare TiO<sub>2</sub> NTs owing to the inactivity of TiO<sub>2</sub> under visible irradiation but it is insufficient to demonstrate the effectiveness of the electrodeposition method, which should be indeed evaluated by photo-catalytic experiments with UV + visible irradiation.

The lower performance of the composite electrodes as compared to the bare TiO<sub>2</sub> may be explained by the exceedingly large size of the Cu<sub>2</sub>O particles (Zhao et al., 2014). To explain this effect, we remark that energy bands undergo bending at the interface between TiO<sub>2</sub> and Cu<sub>2</sub>O and at the interfaces between the two semiconductors (TiO<sub>2</sub> and Cu<sub>2</sub>O) and the electrolyte. Unlike the bending attained at the interface between TiO<sub>2</sub> and Cu<sub>2</sub>O, the bending at the interface between Cu<sub>2</sub>O and the electrolyte can drive the minority carriers

towards the electrolyte and can thus oppose the generation of an anodic current. If the particles size is sufficiently small, the space charge layer at the  $\text{Cu}_2\text{O}$ -electrolyte interface is covered by the space charge layer at the  $\text{Cu}_2\text{O}$ - $\text{TiO}_2$  interface and the influence of  $\text{Cu}_2\text{O}$ -electrolyte interface becomes negligible. However, increasing the particle size, the  $\text{Cu}_2\text{O}$  electrolyte interface can contribute to reduce the photo-generated anodic current.

#### 4. Conclusions

$\text{Ti/TiO}_2/\text{Cu}_2\text{O}$  composite electrodes were produced by electrodeposition of  $\text{Cu}_2\text{O}$  nanoparticles over the surface of  $\text{TiO}_2$  NTs. The application of the composite electrodes to sustain the photo-catalytic degradation of MB and the photo-electrochemical water splitting was evaluated. Despite the deposition of  $\text{Cu}_2\text{O}$  could extend the wavelength range of absorbed radiation to the visible light region, it was found that the photo-catalytic performances of the composite electrodes were lower as compared to the application of the bare  $\text{TiO}_2$  electrode. These results were found to be in agreement with most of the studies addressing the synthesis of  $\text{Cu}_2\text{O}/\text{TiO}_2$  electrodes by  $\text{Cu}_2\text{O}$  electrodeposition over  $\text{TiO}_2$  NTs. The lower performances of the composite as compared to the bare  $\text{TiO}_2$  electrodes could be explained by the exceedingly large size of the electrodeposited nanoparticles. This can enhance the effect of the bending at the  $\text{Cu}_2\text{O}$ -electrolyte interface which can drive electrons towards the electrolyte.

#### References

- Altimari P., Di Caprio F., Toro L., Capriotti A. L., & Pagnanelli F., 2014, Hydrogen photoproduction by mixotrophic cultivation of *Chlamydomonas reinhardtii*: interaction between organic carbon and nitrogen, *Chemical Engineering Transactions*, 38, 199-204.
- Altimari P., Pagnanelli F., 2016, Electrochemical nucleation and three-dimensional growth of metal nanoparticles under mixed kinetic-diffusion control: model development and validation, *Electrochimica Acta*, 206, 116-126.
- Beer C., Reichstein M., Tomelleri E., Ciais P., Jung M., Carvalhais N., Rodenbeck C., Arain M.A., Baldocchi D., Bonan G.B., Bondeau A., Cescatti A., Lasslop G., Lindroth A., Lomas M., Luyssaert S., Margolis H., Oleson K.W., Rouspard O., Veenendaal E., Viovy N., Williams C., Woodward F.I., Papale D., 2010, Terrestrial gross carbon dioxide uptake: global distribution and covariation with climate, *Science*, 329, 834-838.
- Grimes C. A., Mor G. K., 2009, Fabrication of  $\text{TiO}_2$  nanotube arrays by electrochemical anodization: four synthesis generations, Chapter In: *TiO<sub>2</sub> Nanotube Arrays*, Springer, Boston, MA, 1-66.
- Hisatomi T., Kubota J., & Domen K., 2014, Recent advances in semiconductors for photocatalytic and photoelectrochemical water splitting, *Chemical Society Reviews*, 43, 7520-7535.
- Lu Q., Jiao F., 2016, Electrochemical  $\text{CO}_2$  reduction: Electrocatalyst, reaction mechanism, and process engineering, *Nano Energy*, 29, 439-456.
- Macak J. M., Tsuchiya H., Ghicov A., Yasuda K., Hahn R., Baue, S., Schmuki P., 2007,  $\text{TiO}_2$  nanotubes: Self-organized electrochemical formation, properties and applications, *Current Opinion in Solid State and Materials Science*, 11, 3-18.
- Malgras V., Ataee-Esfahani H., Wang H., Jiang B., Li C., Wu K. C. W., Kim J. H., Yamauchi Y., 2016, Nanoarchitectures for mesoporous metals, *Advanced Materials*, 28, 993-1010.
- Momirlan M., & Veziroglu T. N., 2005, The properties of hydrogen as fuel tomorrow in sustainable energy system for a cleaner planet, *International journal of hydrogen energy*, 30, 795-802.
- Sang L., Zhang J., Zhang Y., Zhao Y., & Lin J., 2015, Preparation of  $\text{Cu}_2\text{O}/\text{TiO}_2$  nanotube arrays and their photoelectrochemical properties as hydrogen-evolving photoanode, *Solar Hydrogen and Nanotechnology X*, 9560, 95600M.
- Schiavi P. G., Altimari P., Rubino A., Pagnanelli F., 2018a, Electrodeposition of cobalt nanowires into alumina templates generated by one-step anodization, *Electrochimica Acta*, 259, 711-722.
- Schiavi P. G., Altimari P., Zanon R., Pagnanelli F., 2016, Morphology-controlled synthesis of cobalt nanostructures by facile electrodeposition: transition from hexagonal nanoplatelets to nanoflakes, *Electrochimica Acta*, 220, 405-416.
- Schiavi P. G., Rubino A., Altimari P., Pagnanelli F., 2018b, Two electrodeposition strategies for the morphology-controlled synthesis of cobalt nanostructures, *AIP Conference Proceedings*, 1990, 020005.
- Schiavi P.G., Altimari P., Pagnanelli F., Moscardini E., Toro L., 2015, Synthesis of cobalt nanoparticles by electrodeposition onto aluminium foils, *Chemical Engineering Transactions*, 43, 673-678.
- Zhao L., Dong W., Zheng F., Fang L., & Shen M., 2012, Interrupted growth and photoelectrochemistry of  $\text{Cu}_2\text{O}$  and Cu particles on  $\text{TiO}_2$ , *Electrochimica Acta*, 80, 354-361.